Physical properties of liquid Fe alloys at high pressure and their bearings on the nature of metallic planetary cores

C. Sanloup,[1,2] F. Guyot,[3] P. Gillet,[1] and Y. Fei[4]

Received 17 July 2001; revised 23 March 2002; accepted 30 March 2002; published 5 November 2002.

[1] Sulfur and silicon are among the expected alloying light elements in planetary liquid iron cores. Structural properties of Fe-27 wt % S and Fe-17 wt % Si liquid alloys at high pressure and high temperature (0–5 GPa/1400–2300 K) are measured by synchrotron X-ray diffraction. Sulfur strongly modifies the local structure of liquid iron whereas silicon has only small structural effects. Fe-27 wt % S melts are indeed poorly ordered which explains a higher compressibility compared to pure liquid Fe. These results point out the necessity to consider the strong effect of S on liquid Fe properties while modeling planetary interiors. They imply a low S content in the Earth's outer core, leaving Si as a strong candidate, and argue for a present-day Martian solid core when combined with previous global chemical models. *INDEX TERMS:* 1015 Geochemistry: Composition of the core; 3924 Mineral Physics: High-pressure behavior; 3954 Mineral Physics: X ray, neutron, and electron spectroscopy and diffraction; 6218 Planetology: Solar System Objects: Jovian satellites; 6225 Planetology: Solar System Objects: Mars; *KEYWORDS:* core, liquid, iron, X-rays, Mars, Ganymede

Citation: Sanloup, C., F. Guyot, P. Gillet, and Y. Fei, Physical properties of liquid Fe alloys at high pressure and their bearings on the nature of metallic planetary cores, *J. Geophys. Res.*, *107*(B11), 2272, doi:10.1029/2001JB000808, 2002.

1. Introduction

[2] Light alloying elements have been expected to be present in planetary liquid cores on several grounds. Three major sources of data are used to decipher which is this mixture of light elements: (1) their respective affinity for liquid Fe as a function of P, T, and oxygen fugacity [e.g., *Ohtani et al.*, 1984; *Kato and Ringwood*, 1989; *Goarant et al.*, 1992; *O'Neill et al.*, 1998; *Gessmann et al.*, 2001, and references therein], (2) their presence in iron meteorites, potential analogues of planetary cores or at least of pre-planetary bodies [e.g., *Karato and Murthy*, 1997], and (3) their effect on dynamic properties such as the interfacial tension and the consequent abilities to percolate through a silicate matrix [e.g., *Iida and Guthrie*, 1988; *Dumay and Cramb*, 1995].

[3] The presence of light elements in the terrestrial outer core has been early suggested from seismic data [*Birch*, 1952, 1964] and may be tested soon in the Martian core with the Netlander mission [*Lognonné et al.*, 1998, 2000]. Since the Galileo probe has detected an intrinsic magnetic field in Ganymede [*Schubert et al.*, 1996], requiring a low melting point of core materials, sulfur is also suspected to be present in its core. Indeed, sulfur considerably lowers the melting temperature of iron, and this behavior persists at high pressure [*Brett and Bell*, 1969; *Boehler*, 1992; *Fei et al.*, 1997, 2000], so that Ganymede's core could be in the liquid state in spite of its small size and consequent low amount of internal heat. Meanwhile, it has been proposed that Ganymede may have differentiated recently enough (only 1 Gyr ago) for the core still to be in the liquid state, i.e., not cooled and subsequently solidified yet [*Nagel et al.*, 2000].

[4] We report X-ray diffraction data of liquid Fe-17 wt % Si and Fe-27 wt % S alloys at high pressures up to 6 GPa. The data are interpreted in the light of density measurements of liquid Fe-S alloys at high pressure [*Sanloup et al.*, 2000b] and of a recent investigation of structural changes in liquid Fe at high pressures and high temperatures [*Sanloup et al.*, 2000a].

[5] The experimental data presented in this paper have broad implications for understanding planetary cores. We will discuss (1) the potential nature of the light elements in the terrestrial outer core, (2) the physical state, solid versus liquid, of the Martian core with regard to its moment of inertia, and (3) internal models of small planetary body interiors such as the Galilean satellites.

2. Experimental Techniques

[6] We used a large volume apparatus (Paris-Edinburgh press [*Besson et al.*, 1992; *Mezouar*, 1997] to achieve the *P-T* range of 0–5 GPa and 1400–2300 K while high energy X-ray diffraction data were collected in situ (E = 78.4 keV). Experiments were carried out at the ESRF ID30 synchrotron X-ray beam line (Grenoble, France), with a monochromatic

[1]Laboratoire de Sciences de la Terre, Ecole Normale Supérieure de Lyon, Lyon, France.
[2]Now at Laboratoire Magmatologie et Geochimie Inorganique Experimentale, Université Pierre et Marie Curie, Paris, France.
[3]Laboratoire de Minéralogie-Cristallographie Physique and Institut de Physique du Globe de Paris, Paris, France.
[4]Geophysical Laboratory and Center for High Pressure Research, Carnegie Institution of Washington, D. C., USA.

0148-0227/02/2001JB000808$09.00

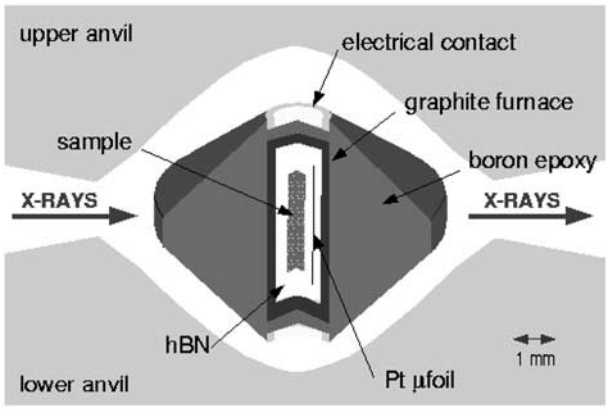

Figure 1. The cell assembly consists of a boron epoxy medium, a graphite furnace, and the sample itself is filling an inner hBN cylinder, acting both as a pressure transmitter and P-T calibrant. The second P-T calibrant is a platinum microfoil (4 μm thick × 0.5 mm width) inserted between two concentric hBN cylinders.

angle dispersive setup (λ = 0.158 Å). The cell assembly (Figure 1) is designed to minimize the absorption of X rays by the furnace (graphite) and the pressure transmitting medium (boron epoxy + hBN). Samples are loaded as pure Fe and Fe-17 wt % Si fine powders or as a mixture of pure Fe and FeS powders. SEM analysis performed on quenched samples attest a posteriori their noncontamination by impurities. Diffraction patterns were collected on Fastscan flat imaging plates [*Thoms et al.*, 1998] from successively the sample (Figure 2), the internal *P-T* calibrants [hexagonal boron nitride (hBN) and platinum], and the sample environment [boron epoxy + hBN] by moving the press perpendicularly to the X-ray beam. The *P-T* conditions were determined within a precision of 50 K and 0.3 GPa from the unit-cell volumes of both internal calibrants which equation of states are known [*Jamieson et al.*, 1982; *Touloukian et al.*, 1977; *Zhao et al.*, 1997]. The unit-cell volume of the calibrants was obtained from their X-ray diffraction pattern using the GSAS program [*Larson and Dreele*, 1994] and selecting diffraction peaks (111), (200), (220) for Pt and (002), (100), (112) for hBN. As attested by the good textural and chemical homogeneity of the recovered samples, temperature gradients in the assembly are less than 10 K/mm [*Mezouar*, 1997].

[7] The observation of diffuse rings with the simultaneous disappearance of crystalline diffraction peaks was used as the criterion to assess complete melting of the sample. After integration of the entire two-dimensional (2-D) imaging plate (Figure 2), the raw 1-D signal was converted into radial distribution functions by Fourier transformation after removing all of the "background" signal including cell assembly (referred to above as the "sample environment") and X-ray Compton scattering. The detailed procedure developed for pure liquid Fe data was described by *Sanloup et al.* [2000a].

3. High-Pressure Experimental Results

[8] X-ray diffraction data on liquid Fe [*Sanloup et al.*, 2000a] allowed the local structure of liquid Fe and its evolution with increasing pressure and temperature to be precisely determined. These data on a relatively simple monoatomic liquid will be used as a reference point for interpreting the structure of the more complex Fe-S and Fe-Si liquid alloys and their deviations from that of pure liquid Fe.

3.1. X-Ray Synchrotron Diffraction Data on Liquid Fe-27 wt % S

[9] We report here the comparison between radial distribution functions of molten Fe and Fe-27 wt % S (Figure 3). Considering an atom in the liquid, the radial distribution function (RDF), $g(r)$, describes the probability of finding another atom in a spherical shell of radius r. Oscillations of $g(r)$ around the $y = 1$ line are therefore a representation of the structure of the liquid. At similar T^*, ($T^* = T/T_m$, T_m: melting temperature), Fe-27 wt % S melts do not present any detectable structure beyond 6 Å, and even the second shell of neighboring atoms (from $\sim$ 4 Å to 5 Å) exhibits a much less structured signal. In this second shell, the difference ($g(r)$-1) in Fe-27 wt % S liquid is indeed close to twice smaller than in both pure Fe and Fe-17 wt % Si liquid at $T^* = 1.15$, and 3 times smaller at higher temperatures. It is consequently very difficult to quantify any pressure effect on the liquid since there is so little structure in the RDF. In contrast, the temperature effect is clearly visible in the second set of atomic shells where the structure is still preserved at $T^* = 1.15$ but becomes barely visible as the temperature increases.

[10] The first neighbor distance is slightly smaller than in pure Fe melt: 2.51–2.52 Å versus 2.56–2.57 Å (Table 1), as already pointed out for much higher pressure conditions by first-principles simulations of liquid Fe-S [*Alfè and Gillan*, 1998]. This effect has been ascribed by *Alfè and Gillan* [1998] to an Fe-S bond stronger than the Fe-Fe one. No S-S bonds, with typical distance of 2 Å [*Winter et al.*, 1990], are observed just below the first Fe-S (or Fe-Fe) distance. Recently, ab initio calculations performed in a P-T range much closer to the one explored here are conforming our results. *Vocadlo et al.* [2000] have calculated Fe-S radial distribution functions at 5 GPa and for 1300–1500 K, the agreement with our experimental curves is excellent (see Figure 3, insert) although the costs of computer time restrain them to the 0–4.5 Å range. These theoretical calculations allow to get the partial distribution functions for S and Fe and confirm the absence of S polymerization because the S-S partial distribution function is basically anticorrelated with the Fe-S radial distribution function.

3.2. X-Ray Synchrotron Diffraction Data on Liquid Fe-17 wt % Si

[11] X-ray diffraction data on liquid Fe-17% Si show that, in contrast to Fe-27 wt % S, this liquid is structurally close to pure liquid Fe (Figure 3), except for a slight compaction toward a higher packed local structure, as observed in the solid state [*Zhang and Guyot*, 1999]. This higher packed local structure is most obvious in the 2nd set of atomic shells. Previous experiments had been conducted at ambient pressure on Fe-Si liquid alloys to measure their density and electrical resistivity [*Gel'd and Gertman*, 1960]. Judging from the shape of the density isotherm, in which clearly two

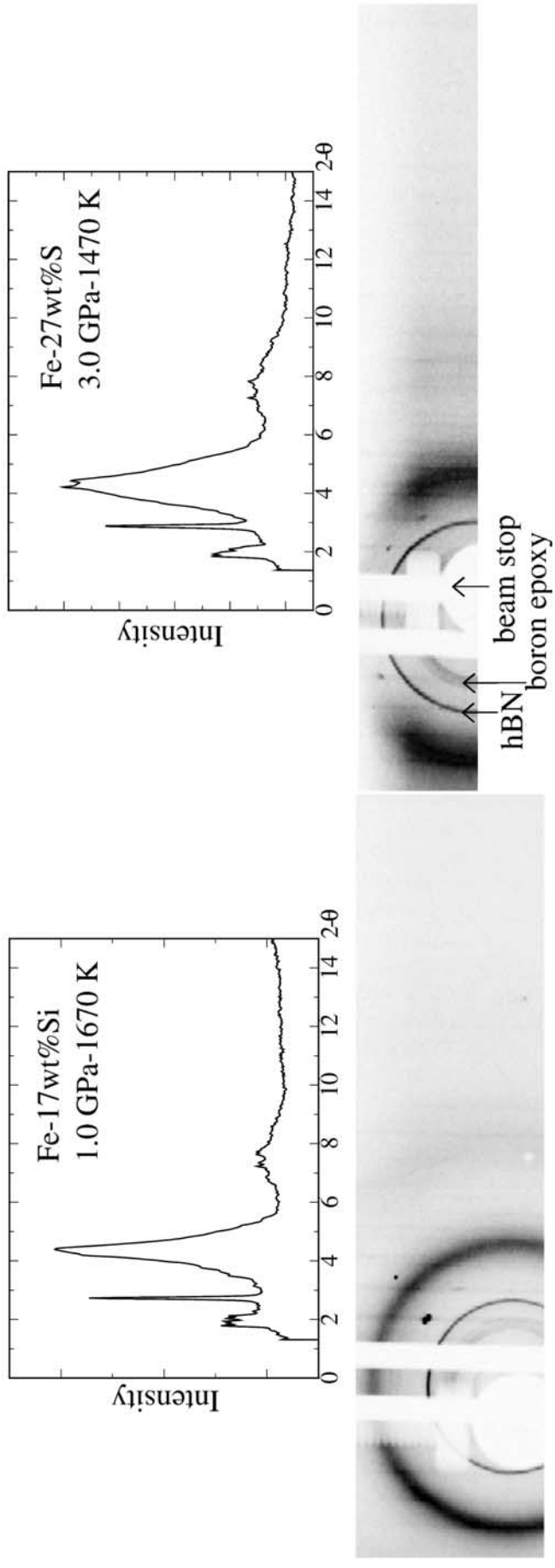

Figure 2. (bottom) Two-dimensional diffraction data collected on imaging plates and (top) the corresponding 1-D integrated patterns. (left) Liquid Fe-17 wt % Si at 1.0 GPa-1670 K and (right) liquid Fe-27 wt % S at 3.0 GPa-1470 K. The white zones correspond to the X-ray beam stop; signal at low angle is due to the boron epoxy gasket, and the next sharp circle is due to the hBN container.

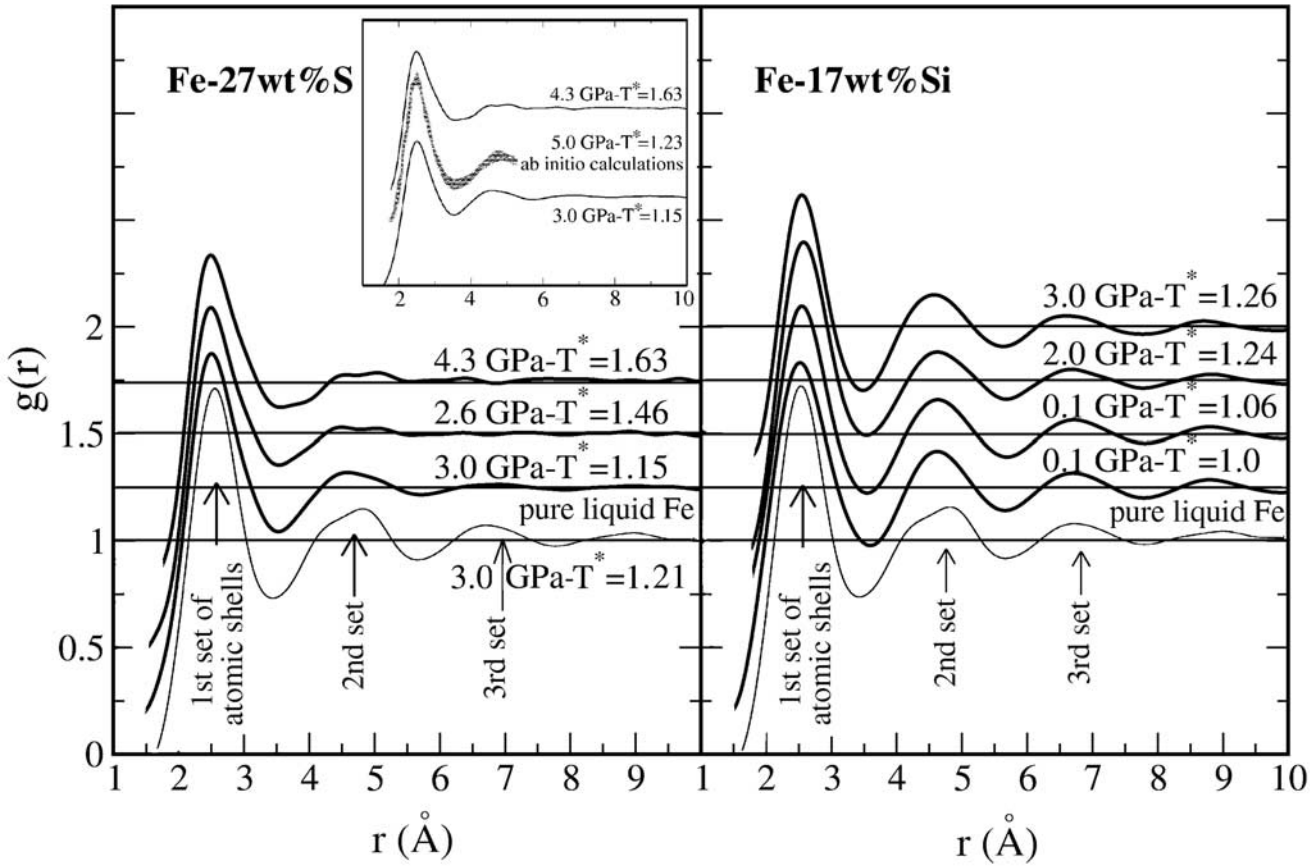

Figure 3. Radial distribution functions for liquid (left) Fe-27 wt % S and (right) Fe-17 wt % Si; insert is displayed $g(r)$ obtained from ab initio calculations [*Vocadlo et al.*, 2000] for comparison with our data obtained at the closest P-T conditions. All $g(r)$ functions have been artificially spaced, and the $y = 1$ line has been added as a guideline.

breaks were displayed, *Gel'd and Gertman* [1960] proposed that groupings related to the tetragonal α-$FeSi_2$ phase and the primitive cubic ε-FeSi phase were present in the melt. Such a coexistence of two types of crystalline-like domains is another structural similarity with pure liquid Fe in which δ-like and γ-like domains coexist in the vicinity of the triple point at 5.2 GPa [*Sanloup et al.*, 2000a].

[12] As for Fe-27 wt % S liquid alloy, the radial distribution functions do not display a distinct contribution from Si-Si partial RDF. In fact, in pure liquid Si, the first distance lies at 2.5 Å [*Petkov*, 1995] and would not be distinguishable from the strong Fe signal in the present data. But the second one, at 3.7 Å in liquid Si, should be observed if it existed since Fe signal is very low in this region, even though Si-Si contributions should be 20 times less intense than Fe-Fe distances in the Fe-17 wt % Si liquid as the diffracted intensity is proportional to Z^2.

[13] Like in pure liquid Fe, variations in $g(r)$ with pressure and/or temperature are observed in the second set of coordination shells. At constant pressure, the second set of atomic shells moves slightly away from the first set with increasing temperature: $(\Delta l_2/l_2 o)/\Delta T = 2.1\ 10^{-5}\ K^{-1}$ at 0.1 GPa and $1.5\ 10^{-5}\ K^{-1}$ at 2.0 GPa. The pressure effect is opposite, with a slight but systematic shortening of

Table 1. Mean Positions for the Integrated First (l_1), Second (l_2), and Third (l_3) Atomic Shells

P/T	l_1[a]	l_2[b]	l_3[c]	CN
Fe				
2300 K–3.0 GPa	2.577 Å (2.685Å)	4.68 Å (1.743)	6.83 Å	10.85
2300 K–4.0 GPa	2.574 Å (–)	4.59 Å (–)	6.71 Å	–
2300 K–5.0 GPa	2.54 Å (2.647 Å)	4.60 Å (1.738)	6.73 Å	11.1
2100 K–3.9 GPa	2.560 Å (2.644 Å)	4.68 Å (1.770)	6.84 Å	11.4
2100 K–4.8 GPa	2.574 Å (2.635 Å)	4.64 Å (1.761)	6.80 Å	11.4
Fe-27 wt % S				
1470 K–3.0 GPa	2.51 Å	4.71 Å (1.88)	–[d]	
1870 K–2.6 GPa	2.51 Å	4.77 Å (1.90)	–[d]	
2090 K–3.6 GPa	2.52 Å	4.73 Å (1.88)	–[d]	
2100 K–4.3 GPa	2.51 Å	4.78 Å (1.90)	–[d]	
Fe-17 wt % Si				
1570 K–0.1 GPa	2.54 Å	4.67 Å (1.88)	6.79 Å	
1670 K–0.1 GPa	2.54 Å	4.68 Å (1.90)	6.78 Å	
1810 K–2.0 GPa	2.54 Å	4.66 Å (1.88)	6.74 Å	
1950 K–2.0 GPa	2.54 Å	4.67 Å (1.90)	6.76 Å	
2040 K–3.0 GPa	2.53 Å	4.63 Å (1.90)	6.69 Å	

[a] Distance at the peak maximum, the integrated mean distance over the first neighbor shell is in parentheses.
[b] Integrated mean position.
[c] Position determined from the midpoint at $g(r) = 1$; the first/second mean distance ratio is in parentheses.
[d] For Fe-27 wt % S melts, there is no significant local order for distances above 5 Å.

the mean position of the second shell while the first set mean distance remains essentially unchanged (Table 1 and Figure 3).

3.3. Comparison With Previous Work

[14] The present diffraction data show that sulfur strongly affects the structure of liquid iron. The number of allowed configurational states in molten Fe-27 wt % S is probably much higher than in pure Fe melt. This result has been predicted from a thermodynamic study of various liquid Fe alloys at ambient pressure [*Shibanova and Vostryakov*, 1990]. The highest value of the entropy of solution, as compared to other metallic alloys (in the Fe-Co-S-Ni-O-Mn-Mg-Zn-Al-Bi-Pb-Ba system), was indeed measured for Fe-S liquid alloys. Such structural data could be related to the chemical diffusivity of both S and Fe, $D \sim 1.\ 10^{-5}$ cm^2 s^{-1} [*Majewski and Walker*, 1998; *Vocadlo et al.*, 2000], because local diffusive motions may control the number of configurational states [*Stebbins*, 1995]. Besides, high- pressure experiments conducted on liquid Fe-S alloys have revealed that the presence of sulfur strongly affects the liquid bulk properties, particularly its compressibility [*Sanloup et al.*, 2000b]. By an X-ray absorption technique, it was shown that increasing the amount of sulfur in liquid iron decreases the bulk incompressibility, K_0, by 2.5 GPa per 1 wt % S, for a planetary S plausible content of 0–20 wt % (Figure 4). The validity of these equations of state has recently been confirmed up to 20 GPa by multianvil experiments based on the sink-float method [*Secco et al.*, 2002]. Structural data obtained in this study on Fe-S alloys therefore provide a rationalized explanation for their large compressibility compared to pure liquid Fe: increasing the number of configurational states adds to the compressibility of the melt by providing additional compression mechanisms.

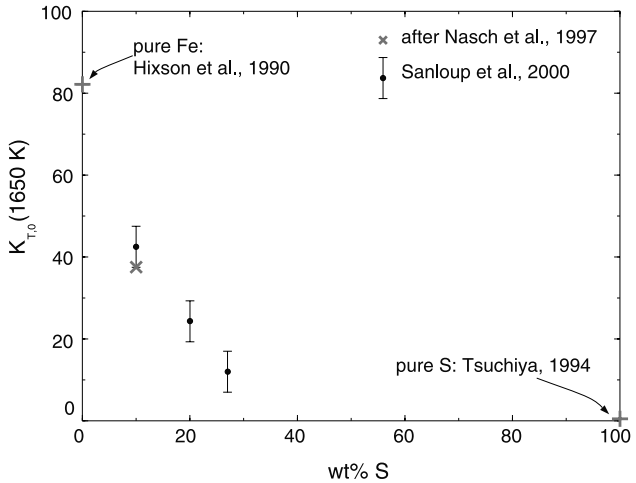

Figure 4. Bulk incompressibility, $K_{T,0}$, as a function of the wt % S content [*Sanloup et al.*, 2000a]. Error bars on $K_{T,0}$ include tests for a 4–7 K'_o range as well as uncertainties on density measurements. Values for pure Fe and pure S were measured by ultrasonic techniques [*Hixson et al.*, 1990; *Tsuchiya*, 1994]. The gray cross represents the $K_{T,0}$ value obtained using the ultrasonic velocity of 3113 m s^{-1} for a Fe-10 wt % S-5 wt % Ni liquid [*Nasch et al.*, 1997] and intersects our measured $K_{T,0}$ range for $K'_o = 7$.

Table 2. Common Characteristics of Martian Models

	Dreibus and Wänke [1985]	*Sanloup et al.* [1999]
Fe/(Mg + Fe)$_{mantle}$	0.75	0.72
M_{core}	0.22	0.23
Weight percent S$_{core}$	14.2	16.2

4. Geophysical Implications

[15] Such a consistency between X-ray absorption data (density measurements) and X-ray diffraction data strengthens our previous results and therefore allows us to address some geophysical issues. Moreover, the observed relationship between the compressibility and the microscopic structure of the liquids can be used to infer qualitatively macroscopic properties from diffraction data only. If ever S is present in non negligible quantities in liquid planetary cores, it can be revealed by comparing both density (density deficit versus pure Fe) and compressibility profiles extracted from seismic data [*Dziewonski and Anderson*, 1981] with such profiles computed using experimental measurements along a relevant geotherm. In contrast, Si would be "invisible" as far as the compressibility is concerned because of similar structure between pure Fe and Fe-Si alloy liquids. The chemical composition of planetary liquid cores should therefore be determined not only from density data, mostly a function of the atomic mass, but also from compressibility data, truly dependent on structural properties.

[16] It may be noted here that nickel is thought to be alloyed to Fe in planetary cores [*Brett*, 1971; *Allègre et al.*, 1995; *Javoy*, 1995], but it does not appreciably change the density of liquid iron or its temperature dependance at ambient pressure: $\rho_{Fe} = -0.65T + 8171.$, while $\rho_{Ni} = -0.64T + 8982.$, for 2000 K < T < 4000 K [*Hixson et al.*, 1990]. We will therefore neglect its effect on liquid iron properties in the following discussion.

[17] In order to model the interiors of planets, our experimental P-T range will need to be extrapolated in the case of terrestrial planets like the Earth and Mars, but it is directly relevant to small planetary bodies (P < 8 GPa).

4.1. Terrestrial Outer Core

[18] Following the original observation by *Birch* [1964], it is now well established that the outer core density and compressibility are close to those of pure liquid Fe [*Anderson and Ahrens*, 1994]. Meanwhile, the density deficit compared to pure liquid Fe amounts to 5–15 wt % [*Jeanloz and Knittle*, 1986; *Laio et al.*, 2000; *Brown and McQueen*, 1982; *Allègre et al.*, 1995; *Javoy*, 1995] and candidate light alloying elements are S, Si, O, C, and H [*Poirier*, 1994]. Decompression of PREM core properties along an adiabatic temperature profile lead to (K_0, K'_0) values for the outer core ranging from (105.3 GPa, 6.42) for a third-order finite strain analysis of PREM velocity to (152.5 GPa, 4.22) for a fourth-order analysis of PREM pressure-density relations [*Jeanloz and Knittle*, 1986]. All of these values are significantly higher than the bulk modulus of pure liquid iron: 85 GPa at 1810 K [*Hixson et al.*, 1990], knowing that K'_0 was

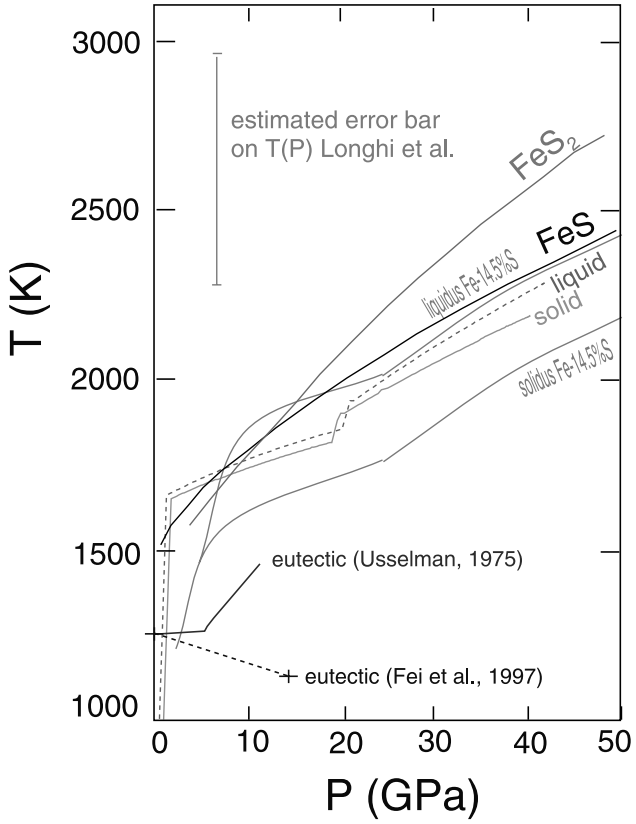

Figure 5. Melting curves [*Boehler*, 1992], eutectic curves [*Usselman*, 1975; *Fei et al.*, 1997] and estimated Martian temperature profiles from *Longhi et al.* [1992] and *Sanloup et al.* [1999] and this work.

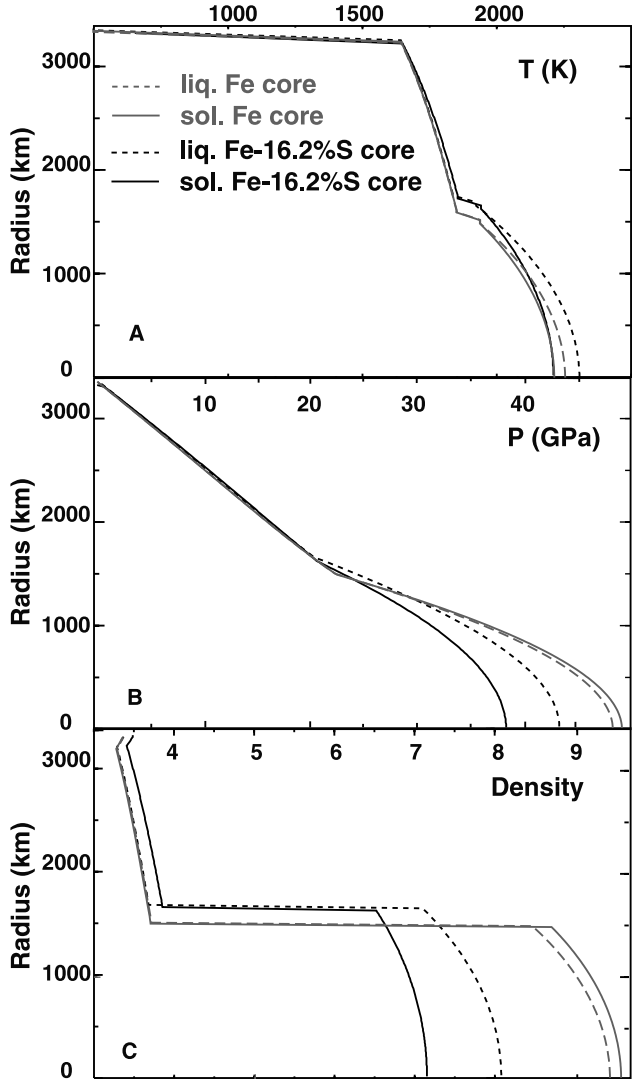

Figure 6. (a) Temperature, (b) pressure, and (c) density profiles for Martian interiors with a solid core (solid line) or a liquid core (dashed line); global composition is chondritic, EH45%–H55% [*Sanloup et al.*, 1999] for the dark curves; gray curves are the same but for a pure Fe core (complete loss of S during accretion).

estimated at 4.66 from a combination of ambient ultrasonic and shock experiments covering the terrestrial pressure range [*Anderson and Ahrens*, 1994]. It was therefore concluded that either the decompression calculations were biased or that structural changes possibly occur in the liquid at high pressure [*Jeanloz and Knittle*, 1986]. This last possibility cannot be ruled out, but so far, it is legitimate to assume that the strong effect that we measured [*Sanloup et al.*, 2000b] of S on K_0 would persist over the megabar pressure range. Through a disordering effect, the alloying of S to liquid Fe in the terrestrial outer core would even increase the discrepancy between the PREM decompressed value [*Jeanloz and Knittle*, 1986] and the experimentally determined value of the bulk modulus. Therefore we propose that sulfur cannot be a major alloying element of the outer core. On the contrary, because Si does not modify the structure of liquid Fe, by means of consequence its bulk properties, it still remains an excellent candidate as a major alloying element in the core. Such a conclusion is consistent with geochemical estimates of the S and Si contents in the core. Based on Zn contents in mantle rocks, S content was estimated to 1.7 wt % [*Dreibus and Palme*, 1996], and global chondritic models predict 2.3 wt % S versus 7.4 wt % Si [*Allègre et al.*, 1995] and 2.6 wt % S versus 10.3 wt % Si [*Javoy*, 1995]. Recent ab initio calculations [*Alfè et al.*,

Table 3. Physical Properties of Martian Models Based on a Global Chondritic Composition[a]

	Solid Fe-16.2 wt % S Core	Liquid Fe-16.2 wt % S Core	Solid Fe Core	Liquid Fe Core
R_c, km	1710 ± 5	1680 ± 5	1510 ± 5	1515 ± 5
ρ_o mantle	3445 ± 5	3380 ± 5	3350 ± 5	3360 ± 5
ρ_o core, kg m^{-3}	6895 ± 10 (at 1400 K)	6274 ± 10 (at 1650 K)	7650 ± 10 (at 1400 K)	7115 ± 10 (at 1650 K)
I/MR^2	0.363	0.356	0.353	0.354

[a] From *Sanloup et al.* [1999]; M_c, the core mass, is 23 wt % for a Fe-16.2 wt % S core and 20 wt % for a pure Fe core, crustal thickness is 20 km (ρ_{crust} = 3000 kg m^{-3}) and K_{mantle} = 130 GPa.

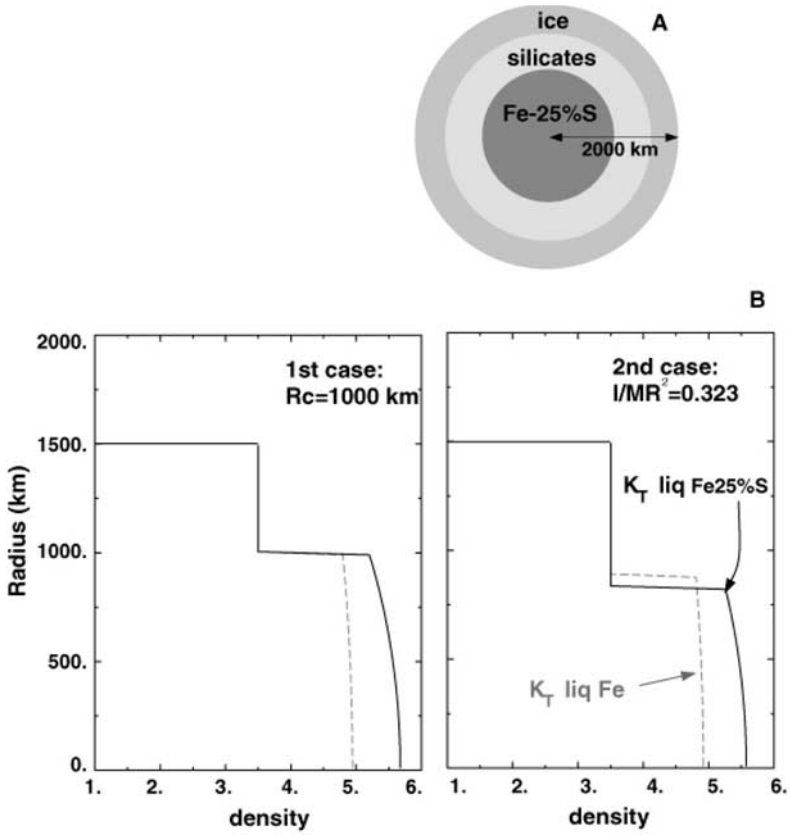

Figure 7. (a) Schematic interiors of a small imaginary planet; and (b) density profiles taking into account the sulfur effect on K_T in the equation of state for a liquid (solid line) or a solid (dashed line) Fe-25 wt % S core.

2000] provide strong evidence against a large S content in the terrestrial outer core as well. Indeed, the authors calculate that the S atomic volume is almost identical to that of Fe, and therefore predict a density difference of only 2.5% at the inner core boundary for a binary Fe-S mixture (8 wt % S). From the convergence of geochemical data and ab initio calculations, it appears that the most likely explanation is that there is a very small amount of S, if any, in the outer core, leaving Si as a main candidate.

4.2. Mars: Solid or Liquid Core?

[19] Available models of the interior of Mars are based on element correlations in SNC meteorites combined with a global CI chondrite content for both refractory elements and Fe [*Dreibus and Wänke*, 1985] and oxygen isotopic composition of the SNC meteorites [*Sanloup et al.*, 1999]. Though deriving from different initial assumptions, these models agree on several points: a high Fe/(Fe + Mg) content in the mantle and a high sulfur content in the core (Table 2). The evolution of temperature with depth is very difficult to predict for Mars, no heat flow data are available and most models either assume an adiabatic temperature profile starting from an assumed lithospheric depth [*Schubert et al.*, 1992; *Sanloup et al.*, 1999], or extract a temperature profile from convection codes applied to the Martian mantle [*Mocquet et al.*, 1996; *Breuer et al.*, 1997]. The resulting $\Delta T(z)$ between several models is 500 K. This uncertainty combined with the uncertainties on Fe-S melting and eutectic curves at high pressure prevents us from answering the question of the Martian core present-day state (Figure 5), even though paleomagnetic crustal features suggest a liquid core in the past [*Connerney et al.*, 1999]. Deciding whether or not the core is liquid on the ground of the calculated Martian geotherms is difficult due to the uncertainties on the temperature profiles and to the uncertainties on the core composition, i.e., on the eutectic depression of liquid Fe by the alloying element(s). Therefore, modeling Mars's interior in both cases, i.e., solid versus liquid core, and comparing the calculated moment of inertia with its observed value may help to resolve this question.

[20] In previous models [*Longhi et al.*, 1992; *Bertka and Fei*, 1998a, 1998b; *Sanloup et al.*, 1999], the Martian core was assumed to be solid, or at least, the elastic properties used for computing core density profiles corresponded to solid Fe-FeS phases. This assumption was directly related to the non availability of equations of state for liquid Fe-x%S alloys. Since such equations of state have now been experimentally determined [*Sanloup et al.*, 2000b], modeling of Martian interiors can now also be done considering a liquid core. To quantify the S effect on the planet's properties, we assumed a chondritic EH45 wt %–H55 wt % bulk composition [*Sanloup et al.*, 1999]; the S effect would be the same for any other bulk composition as long as there is a nonnegligible S content in the core. Calculations were also carried out for a S-free core, as S loss during planetary accretion may have occurred although being very difficult to estimate. Results of the calculations for the moment of inertia (in its dimensionless form), the zero pressure density

of mantle materials and their iron number (Fe/(Fe + Mg)) are displayed in Tables 2 and 3. The most important difference concerns the moment of inertia: 0.363 for a solid Fe-Ni-16.2 wt % S core versus 0.356 for a liquid Fe-Ni-16.2 wt % S core. Indeed, for a constant core mass of 23% (as derived from the global chemical composition of 45% EH chondrites–55% H chondrites without S loss), considering a liquid core implies a higher compressibility of core materials, that is a concentration of larger densities toward the rotation axis and, consequently, a redistribution of masses in the mantle (Figure 6c). Assuming a total loss of S during accretion reduces the effect of considering a solid versus liquid core but in these S-free core cases, the predicted moment of inertia is even lower than in both previous cases. Since the recent Martian missions, Mars Pathfinder and Mars Global Surveyor, the moment of inertia has been more precisely determined, at 0.365 ± 0.02 [*Folkner et al.*, 1997; *Smith et al.*, 1999]. Moreover, the lighter mantellic ρ_o, 3380 kg m^{-3} in the case of a liquid core, is not consistent with the magnesium number combined with the mantellic normative mineralogical composition which implies a density close to 3450 kg m^{-3} [*Sanloup et al.*, 1999].

[21] Therefore the new data obtained on Fe-S liquid alloys tend to favor a solid state for the Martian core. Mars core materials could thus be close to the newly discovered Fe_3S phase [*Fei et al.*, 2000] with 16.1 wt % S, close to the Martian core composition (Table 2) and stable above 18 GPa (Figure 6b).

4.3. Models of Cores of Small Planets

[22] Our experimental pressure conditions (density and structure of liquid Fe alloys) are directly relevant to the interior of a small planet, 2000-km in radius size, that is, typically, a Galilean satellite. The question we address here, is whether or not it is important to consider the S effect on the equation of state of potential core materials. In the case of Galilean satellites, if ever some of them do possess a liquid metallic core [*Schubert et al.*, 1996], then the molten state is more easily achieved for a eutectic Fe-FeS composition, which is close to Fe-25 wt % S for a 4–8 GPa pressure range [*Usselman*, 1975].

[23] We therefore calculate a density profile through an imaginary planet, considering a stepwise profile in the outer icy and silicate shells, and inverting a Birch-Murnaghan equation of state for the core. In a first case, core size and density profiles for the three reservoirs (core, silicate mantle, ice crust) are fixed to quantify the S effect in modeling the core mass and the moment of inertia. Results are displayed on Figure 7. The mean core density, and consequently the core mass, is 10% higher if the effect of sulfur on K_T, the bulk incompressibility, is considered (S lowers K_T and consequently, ρ increases more strongly with pressure). It also follows that the dimensionless moment of inertia, I/MR^2, will be 1% higher as more mass is added close to the center of the planet. We emphasize that in contrast to the Martian case (see section 4.2), we are not working with a constant total mass but instead, with constant core size so that no redistribution of mass occurs in the outer shells. Currently, this last result is not a decisive one for modeling the interiors of Galilean satellites since the error bars on I/MR^2 are also 1% as determined from the recent Galileo mission [*Anderson et al.*, 1998]. In a second case, we quantify the S effect on the core size, by fixing the moment of inertia ($I/MR^2 = 0.323$) and considering the same stepwise density profile for the outer shells as in the first case. The calculated core size while using $K_{T,FeS}$, 830 km, is 55 km smaller than while neglecting the S effect on the equation of state, i.e., using $K_{T,Fe}$; accounting for the S effect in this constant I/MR^2 case again increases the core mass by 10%.

[24] The strong effect of sulfur on the compressibility of liquid Fe should thus be taken into account in the modeling of cores of small planets from astronomical data.

5. Conclusions

[25] Synchrotron X-ray structural data acquired at high pressure (up to 5 GPa) have revealed very different radial distribution functions for liquid Fe-27 wt % S and Fe-17 wt % Si alloys. Fe-27 wt % S melts are poorly structured which explains a very high compressibility compared to pure liquid Fe. In contrast, Si is "invisible" as far as compressibility is concerned and its presence will be probed only by density profiles. Indeed, Fe-17 wt % Si melts display an Fe-like local order, probably resulting in very close macroscopic properties such as the bulk compressibility. As Fe-S melts behave so differently from Fe-Si melts, it follows that if ever S is present in a liquid planetary core, then (1) S will be detected even in relatively small quantities and (2) we do need to consider its strong effect on core materials' properties (namely their equations of state). The same is true for the difference between Fe-S melt and Fe-S solid properties. That is, we can test the solid versus liquid state of a planetary core, for instance the Martian core, by modeling the interior of Mars. Different planetary characteristics are indeed calculated depending on the chosen core state. Regarding the moment of inertia, our density data favor a solid state for the Martian core.

[26] **Acknowledgments.** The authors thank M. Mezouar, G. Fiquet, and I. Martinez for their help during the experiments on liquid iron alloys at the European Synchrotron Radiation Facility and anonymous referees for their useful comments which helped to improve the quality of the manuscript.

References

Alfè, D., and M. J. Gillan, First-principle simulations of liquid Fe-S under Earth's conditions, *Phys. Rev. B*, *58*, 8248–8256, 1998.

Alfè, D., M. J. Gillan, and G. D. Price, Constraints on the composition of the Earth's core from ab initio calculations, *Nature*, *405*, 172–175, 2000.

Allègre, C.-J., J.-P. Poirier, E. Humler, and A. W. Hofmann, The chemical composition of the Earth, *Earth Planet. Sci. Lett.*, *134*, 515–526, 1995.

Anderson, J. D., G. Schubert, R. A. Jacobson, E. Lau, W. B. Moore, and W. L. Sjogren, Europa's differentiated internal structure: Interferences from four Galileo encounters, *Science*, *281*, 2019–2021, 1998.

Anderson, W. W., and T. J. Ahrens, An equation of state for liquid iron and implications for the Earth's core, *J. Geophys. Res.*, *99*, 4273–4284, 1994.

Bertka, C. M., and Y. Fei, Density profile of an SNC model Martian interior and the moment of inertia factor of Mars, *Earth Planet. Sci. Lett.*, *157*, 79–88, 1998a.

Bertka, C. M., and Y. Fei, Implication of Mars Pathfinder data for the accretion history of the terrestrial planets, *Science*, *281*, 1838–1840, 1998b.

Besson, J. M., G. Hamel, T. Grima, R. J. Nelmes, J. S. Loveday, S. Hull, and D. Häusermann, A large volume pressure cell for high temperatures, *High Pressure Res.*, *8*, 625–630, 1992.

Birch, F., Elasticity and constitution of the Earth's interior, *J. Geophys. Res.*, *57*, 227–286, 1952.

Birch, F., Density and composition of mantle and core, *J. Geophys. Res.*, *69*, 4377–4388, 1964.

Boehler, R., Melting of the Fe-FeO and the Fe-FeS systems at high pres-

sure: Constraints on core temperature, *Earth Planet. Sci. Lett.*, *111*, 217–227, 1992.
Brett, R., The Earth's core: Speculations on its chemical equilibrium with the mantle, *Geochim. Cosmochim. Acta*, *35*, 203–221, 1971.
Brett, R., and P. M. Bell, Melting relations in the Fe-rich portion of the system Fe-FeS at 30 kb pressure, *Earth Planet. Sci. Lett.*, *6*, 479–482, 1969.
Breuer, D., D. A. Yuen, and T. Spohn, Phase transitions in the martian mantle: Implications for partially layered convection, *Earth Planet. Sci. Lett.*, *148*, 457–470, 1997.
Brown, J. M., and R. G. McQueen, The equation of state for iron and the Earth's core, in *High-Pressure Research in Geophysics*, pp. 611–623, Cent. for Acad. Publ. Jpn., Tokyo, 1982.
Connerney, J. E. P., M. H. Acuña, P. J. Wasilewski, N. F. Ness, H. Rème, C. Mazelle, D. Vignes, R. P. Lin, D. L. Mitchell, and P. A. Cloutier, Magnetic lineations in the ancient crust of Mars, *Science*, *284*, 794–798, 1999.
Dreibus, G., and H. Palme, Cosmochemical constraints on the sulfur content in the Earth's core, *Geochim. Cosmochim. Acta*, *60*, 1125–1130, 1996.
Dreibus, G., and H. Wänke, A volatile-rich planet, *Meteoritics*, *20*, 367–382, 1985.
Dumay, C., and A. W. Cramb, Density and interfacial tension of liquid Fe-Si alloys, *Metall. Trans. B*, *26*, 173–176, 1995.
Dziewonski, A. M., and D. L. Anderson, Preliminary reference Earth model, *Phys. Earth Planet. Inter.*, *25*, 297–356, 1981.
Fei, Y., C. M. Bertka, and L. W. Finger, High-pressure iron-sulfur compound, Fe_3S_2, and melting relations in the system Fe-FeS at high pressure, *Science*, *275*, 1621–1624, 1997.
Fei, Y., J. Li, C. M. Bertka, and C. T. Prewitt, Structure type and bulk modulus of Fe_3S, a new iron-sulfur compound, *Am. Mineral.*, *85*, 1830–1833, 2000.
Folkner, W. M., C. F. Yoder, D. N. Yuan, E. M. Standish, and R. A. Preston, Interior structure and seasonal mass redistribution of Mars from radio tracking of Mars Pathfinder, *Science*, *278*, 1749–1752, 1997.
Gel'd, P. V., and Y. M. Gertman, On the interparticle interaction in liquid alloys of silicon with iron and nickel, in *Structure and Properties of Liquid Metals*, pp. 181–185, Russ. Acad. of Sci., Moscow, 1960.
Gessmann, C. K., B. J. Wood, D. C. Rubie, and M. R. Kilburn, Solubility of silicon in liquid metal at high pressure: Implications for the composition of the Earth's core, *Earth Planet. Sci. Lett.*, *184*, 367–376, 2001.
Goarant, F., F. Guyot, and J.-P. Poirier, High-pressure and high-temperature reactions between silicates and liquid iron alloys, in the diamond anvil cell, studied by analytical electron microscopy, *J. Geophys. Res.*, *97*, 4477–4487, 1992.
Hixson, R. S., M. A. Winkler, and M. L. Hodgon, Sound speed and thermophysical properties of liquid iron and nickel, *Phys. Rev. B*, *42*, 6485–6491, 1990.
Iida, T., and R. I. L. Guthrie, *The Physical Properties of the Liquid Metals*, Clarendon, Oxford, England, 1988.
Jamieson, J. C., J. N. Fritz, and M. H. Anghnani, Pressure measurement at high temperature in X-ray diffraction studies: Gold as a primary standard, *High Pressure Res.*, *12*, 27–48, 1982.
Javoy, M., The integral enstatite chondrite model of the Earth, *Geophys. Res. Lett.*, *22*, 2219–2222, 1995.
Jeanloz, R., and E. Knittle, Reduction of mantle and core properties to a standard state by adiabatic decompression, in *Advances in Physical Geochemistry*, pp. 275–309, Springer-Verlag, New York, 1986.
Karato, S.-I., and V. R. Murthy, Core formation and chemical equilibrium in the Earth, I, Physical considerations, *Phys. Earth Planet. Inter.*, *100*, 61–79, 1997.
Kato, T., and A. E. Ringwood, Melting relationships in the system Fe-FeO at high pressures: Implications for the composition and formation of the Earth's core, *Phys. Chem. Miner.*, *16*, 524–538, 1989.
Laio, A., S. Bernard, G. L. Chiarotti, S. Scandolo, and E. Tosatti, Physics of iron at Earth's core conditions, *Science*, *287*, 1027–1030, 2000.
Larson, A., and R. V. Dreele, Gsas manual, *LAUR Publ. 86-748*, pp. 86–748, Los Alamos Natl. Lab., Los Alamos, N. M.1994.
Lognonné, P., et al., The seismic Optimism experiment, *Planet. Space Sci.*, *46*, 739–747, 1998.
Lognonné, P., A. M. Harri, O. Marsal, J. L. Counil, T. Spohn, and the Netlander Team, The Netlander Mission, in *Geophysical Research Abstracts, EGS 25th General Assembly*, vol. 2, Eur. Geophys. Soc., Katlenburg-Lindau, Germany, 2000.
Longhi, J., E. Knittle, and J. R. Holloway, The bulk composition, mineralogy and internal structure of Mars, in *Mars, Space Sci. Ser.*, vol. 20, pp. 184–208. Univ. of Ariz. Press, Tucson, 1992.
Majewski, E., and D. Walker, S diffusivity in Fe-Ni-S-P melts, *Earth Planet. Sci. Lett.*, *160*, 823–830, 1998.
Mezouar, M., Etude du diagramme de phase de l'antimoniure d'indium InSb sous hautes pression et température, Ph.D. thesis, Univ. Paris VII, Paris, 1997.
Mocquet, A., P. Vacher, O. Grasset, and C. Sotin, Theoretical seismic models of Mars: The importance of the iron content of the mantle, *Planet. Space*, 44, 1996.
Nagel, K., D. Breuer, and T. Spohn, Differentiation of Callisto and Ganymede, in *Geophysical Research Abstracts, EGS 25th General Assembly, vol. 2*, Eur. Geophys. Soc., Katlenburg-Lindau, Germany, 2000.
Nasch, P. M., M. H. Manghnani, and R. A. Secco, Anomalous behaviour of sound velocity and attenuation in liquid Fe-Ni-S, *Science*, *277*, 219–221, 1997.
Ohtani, E., A. E. Ringwood, and W. Hibberson, Composition of the core, II, Effect of high pressures on the solubility of FeO in molten iron, *Earth Planet. Sci. Lett.*, *71*, 94–103, 1984.
O'Neill, H. S. C., D. Canil, and D. C. Rubie, Oxide-metal equilibria to 2500°C and 25 GPa: Implications for core formation and the light component in the Earth's core, *J. Geophys. Res.*, *103*, 12,239–12,260, 1998.
Petkov, V., Atomic ordering in liquid Si and Ge by structural diffusion model calculations, *J. Phys. Condens. Matter*, *7*, 5745–5752, 1995.
Poirier, J.-P., Physical properties of the Earth's core, *Phys. Earth Planet. Inter.*, *85*, 319–337, 1994.
Sanloup, C., A. Jambon, and P. Gillet, A simple chondritic model for Mars, *Phys. Earth Planet. Inter.*, *112*, 41–52, 1999.
Sanloup, C., F. Guyot, P. Gillet, G. Fiquet, R. Hemley, M. Mezouar, and I. Martinez, Structural changes in liquid Fe at high pressures and high temperatures from synchrotron x-ray diffraction, *Europhys. Lett.*, *52*, 151–157, 2000a.
Sanloup, C., F. Guyot, P. Gillet, G. Fiquet, M. Mezouar, and I. Martinez, Density measurements of liquid Fe-S alloys at high-pressure, *Geophys. Res. Lett.*, *27*, 811–814, 2000b.
Schubert, G., S. C. Solomon, D. L. Turcotte, M. J. Drake, and N. H. Sleep, Origin and thermal evolution of Mars, in *Mars, Space Sci. Ser.*, vol. 20, pp. 147–183, Univ. of Ariz. Press, Tucson, 1992.
Schubert, G., K. Zhang, M. G. Kivelson, and J. D. Anderson, The magnetic field and internal structure of Ganymede, *Nature*, *384*, 544–545, 1996.
Secco, R., M. D. Rutter, S. P. Balog, H. Liu, D. C. Rubie, T. Uchida, D. Frost, Y. Wang, M. Rivers, and S. R. Sutton, Viscosity and density of Fe-S liquids at high pressures, paper presented at AIRAPT-18, *J. Phys. Condens. Matter*, in press, 2002.
Shibanova, L. N., and A. A. Vostryakov, Entropy of solution of oxygen and sulfur in liquid, binary, metal alloys, *Izv. Akad. Nauk SSSR Neorg. Mater.*, *27*, 2570–2573, 1990.
Smith, D., et al., The global topography of Mars and implications for surface evolution, *Science*, *284*, 1495–1503, 1999.
Stebbins, J. F., Dynamics and structure of silicate and oxide, in *Structure, Dynamics and Properties of Silicate Melts, Rev. Mineral*, vol. 32, edited by J. Stebbins, P. F. McMillan, and D. B. Dingwell, pp. 191–246, Mineral. Soc. of Am., Washington, D. C., 1995.
Thoms, M., D. Häusermann, S. Bauchau, M. Kunz, T. LeBihan, M. Mezouar, and D. Strawbridge, An improved detector for use at synchrotrons, *Nucl. Instrum. Methods*, *413*, 175, 1998.
Touloukian, Y. S., R. K. Kirby, R. E. Taylor, and T. Y. R. Lee, (Eds.), *Thermophysical Properties of Matter*, vol. 13, Plenum, New York, 1977.
Tsuchiya, Y., The thermodynamics of structural changes in the liquid sulphur-tellurium system: Compressibility and Ehrenfest's relations, *J. Phys. Condens. Matter*, *6*, 2451–2458, 1994.
Usselman, T. M., Experimental approach to the state of the core: Part I. The liquidus relations of the Fe-rich portion of the Fe-Ni-S system from 30 to 100 kb, *Am. J. Sci.*, *275*, 278–290, 1975.
Vocadlo, L., D. Alfè, G. D. Price, and M. J. Gillan, First principles calculations on the diffusivity and viscosity of liquid Fe-S at experimentally accessible conditions, *Phys. Earth Planet. Inter.*, *120*, 145–152, 2000.
Winter, R., P. A. Egelstaff, W.-C. Pilgrim, and W. S. Howells, The structural properties of liquid, solid and amorphous sulfur, *J. Phys. Condens. Matter*, *2*, 215–218, 1990.
Zhang, J., and F. Guyot, Thermal equation of state and $Fe_{0.91}Si_{0.09}$, *Phys. Chem. Miner.*, *26*, 206–211, 1999.
Zhao, Y. S., R. B. V. Dreele, T. J. Shankland, D. J. Weidner, J. Z. Zhang, Y. B. Wang, and T. Gasparik, P-V-T data of hexagonal boron nitride hBN and determination of pressure and temperature using thermoelastic equations of state of multiple phases, *High Pressure Res.*, *15*, 369–386, 1997.

Y. Fei, Geophysical Laboratory and Center for High Pressure Research, Carnegie Institution of Washington, 5251 Broad Branch Road, N.W., Washington, DC 20015, USA. (fei@gl.ciw.edu)
P. Gillet, Ecole Normale Supérieure de Lyon, F-69364 Lyon cedex 07, France. (pgillet@ens-lyon.fr)
F. Guyot, Laboratoire de Minéralogie-Cristallographie Physique and Institut de Physique du Globe de Paris, 4, place Jussieu, F-75252 Paris cedex 05, France. (francois.guyot@lmcp.jussieu.fr)
C. Sanloup, Laboratoire MAGIE, Université Pierre et Marie Curie, case 110, F-75252 Paris cedex 05, France. (sanloup@ccr.jussieu.fr)